

New compounds of p-block elements by high-pressure synthesis

Ulrich Schwarz[#], Lev Akselrud, Matej Bobnar, Ulrich Burkhardt, Kai Guo, Julia Hübner, Marcus Schmidt, Alexandra Zevalkink

Pressure is a fundamental state variable and as such a versatile tool to yield novel structural motifs with unusual chemical environments and bonding situations. Despite the already rich structure chemistry of p-block main group elements, the realization of novel structure patterns by compression gives rise to fascinating modifications of the chemical bonding which frequently set the stage for intriguing physical properties like superconductivity.

The quest for new materials is frequently connected with the realization of structure patterns with unique composition and spatial arrangement of the components. A most versatile tool for the manufacture of unusual motifs is the application of hydrostatic pressure as one of the fundamental thermodynamic state variables. In such a way, compression represents an effective means to manipulate the stability of phases and to assemble new inorganic compounds for materials chemistry. The beneficial effects of pressure for yielding metastable compounds are not limited to systems which exhibit pronounced miscibility gaps, but also cover the suppression of evaporation losses as well as the stabilization of patterns with increased coordination numbers.

Following a theoretical prediction, mixtures of ^{57}Fe or $\zeta\text{-}^{57}\text{Fe}_2\text{N}$ with condensed nitrogen were laser-heated at pressures up to 45 GPa. Heating to 1300 K at pressures above 10 GPa resulted in the formation of a new phase [1] exhibiting moderate hyperfine splitting (Figure 1). The magnetic splitting is observed up to 45 GPa, the highest pressure of the present investigation, indicating robust magnetic order of the new phase. Annealing at the same temperature below 10 GPa induces the transformation of the new phase into $\zeta\text{-}^{57}\text{Fe}_2\text{N}$. The crystal structure of NiAs-type ^{57}FeN was refined using synchrotron X-ray diffraction data recorded at 13.3 GPa. The structure pattern comprises iron-iron contacts along [001], i.e. parallel to the c-axis, which essentially correspond to those of elemental iron, $\varepsilon\text{-Fe}$. *Ab initio* band structure calculations for the new phase give evidence that the pattern is crucially stabilized by magnetic ordering of the metal atoms. The magnetic properties of the phase are also clearly evidenced by the observed multiplet in the Moessbauer data [1].

While earlier efforts on binary phases of the heavier group homologue bismuth with various transition metals were focused on systems exhibiting miscibility gaps, the binary mixtures with copper show eutectic behaviour, i.e., the metals can be combined in a wide

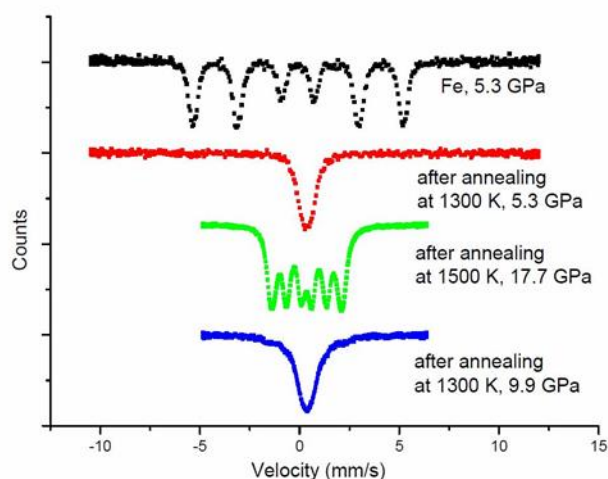


Figure-1: ^{57}Fe -Mössbauer spectra of the selected iron-nitrogen mixtures at various pressures [1]. Black: ^{57}Fe in nitrogen. Red: After laser-heating at 5.3 GPa, the spectrum indicates known iron nitrides. Green: After laser-heating at 17.7 GPa, the multiplet is dominated by the signal of the new phase. Blue: Spectrum evidencing the decomposition into the known nitrogen-poorer compounds of iron [1].

range of compositions, but do not form discrete compounds. However, upon application of $P = 5$ GPa and $T = 720$ K, the compound CuBi is formed [2].

An analysis of the chemical bonding in CuBi by the QTAIM (quantum theory of atoms in molecules) and the ELI (electron localizability indicator) technique indicates that the bonding interactions in CuBi are essentially non-polar.

The ELI analysis reveals three types of multicentre bonds (Figure 2). The first connects one Bi and three Cu atoms within a tetrahedron, thus indicating a four-centre interaction (Figure 2, light yellow isosurface). The second type of four-centre bond is also located within a tetrahedron of Bi and three copper atoms (dark yellow ELI-D isosurface in Figure 2). The dark orange ELI-D isosurface indicates stereochemically active lone-pairs at bismuth.

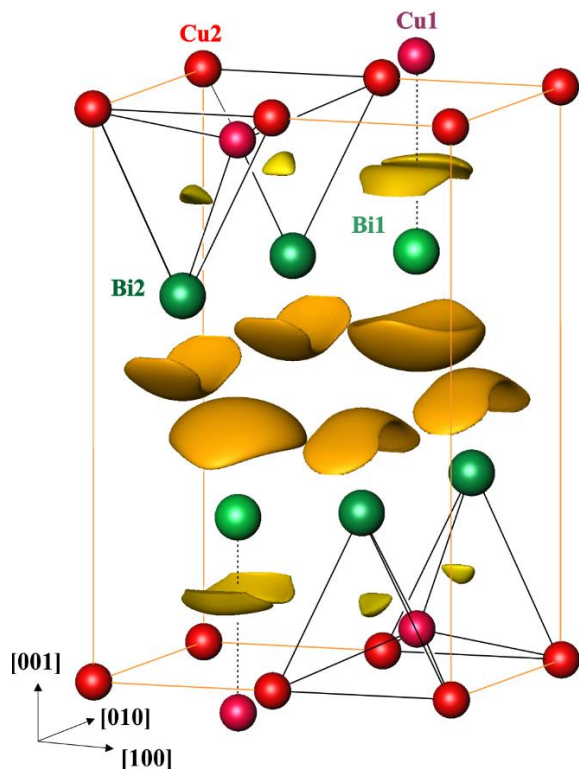


Figure-2: Electron localizability indicator (U , ELI-D) in hp -CuBi [2]. The isosurfaces with $U = 0.9775$ (light yellow) and $U = 1.002$ (dark yellow) visualize $4c$ interactions Bi-Cu-Cu-Cu, the one with $U = 1.082$ (orange) reveals lone-pairs on both types of Bi atoms. Thin orange lines show the unit cell; thin black lines connect the atoms participating in the four-centre bonding [2].

Several metallic bismuth compounds exhibit superconducting transitions at low temperatures (Figure 3). The critical temperature of compounds containing the $4d$ metal rhodium are significantly higher than those of the lighter $3d$ metals copper and

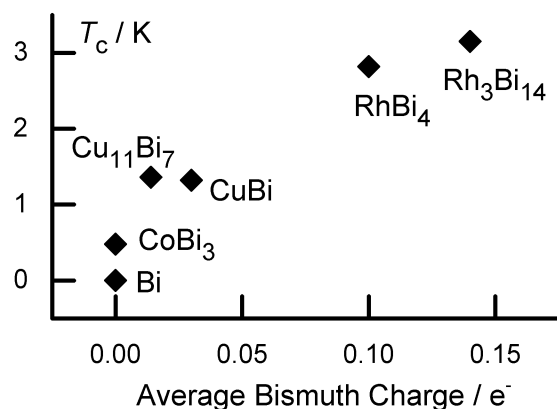


Figure-3: Critical superconducting temperature for bismuth and its compounds vs. the average charge transfer per one Bi atom [2].

cobalt. Within the BCS theory, reduction of the average atomic mass causes higher critical temperatures. This is not found for the investigated superconducting bismuth compounds. Instead, data evidence an increase of the transition temperature with growing average charge transfer (Figure 3).

The quest for new covalent intermetallic compounds of silicon or germanium already led to the high-pressure synthesis of several structural patterns with tetrel-rich composition. In the class of rare earth metals, lutetium is of special interest as a component as it provides absence of a magnetic momentum in the usual oxidation state +3.

The new germanide LuGe₃ [3] was prepared by high-pressure high-temperature synthesis at pressures between 8(1) and 14(2) GPa and temperatures ranging from 1100(150) to 1500(150) K. LuGe₃ crystallizes in a DyGe₃-type structure. While two types of germanium atoms (Ge2 and Ge3) constitute double layers of condensed Ge₂-dumbbells, a third type of Ge atom (Ge1) forms zigzag chains between these 2D units.

Analysis of the electron localizability indicator (ELI-D) (Figure 4) reveals the absence of ELI-D maxima visualizing the outer (valence) shell of Lu evidencing cationic behaviour of the metal. The second characteristic feature is the presence of ELI-D maxima around the Ge cores.

The Ge1 atoms in the zigzag chains are characterized by two bonds to neighbouring germanium atoms plus lone-pair-like features. The ELI-D distribution around the dumbbell atoms Ge2 and Ge3 indicates covalent bonding within the Ge₂ units plus two other attractors on the outer sides (Figure 4, top). The real bonding pattern is more complex as there are additional bonds between the dumbbells in the (010) planes (Figure 4, middle). The bonds in the chains are two-centre interactions, but involve only 0.7 electrons each (Figure 4, bottom, red basin). The dumbbell bonds have 2c character and comprise two electrons (figure 4, bottom, pink basin). Additionally, each of these germanium atoms shows lone-pair-like basins containing about two electrons. These have common surfaces with the lutetium cores and visualize rather polar multicentre interactions (Figure 4, bottom, blue, pink and green basins).

The electrical resistivity $\rho(T)$ of LuGe₃ (Figure 5) shows a positive slope, denoting metallic behaviour being well-described within the Bloch-Grüneisen model. At zero-field a drop indicates the transition into a superconducting state at $T_c = 3.6$ K.

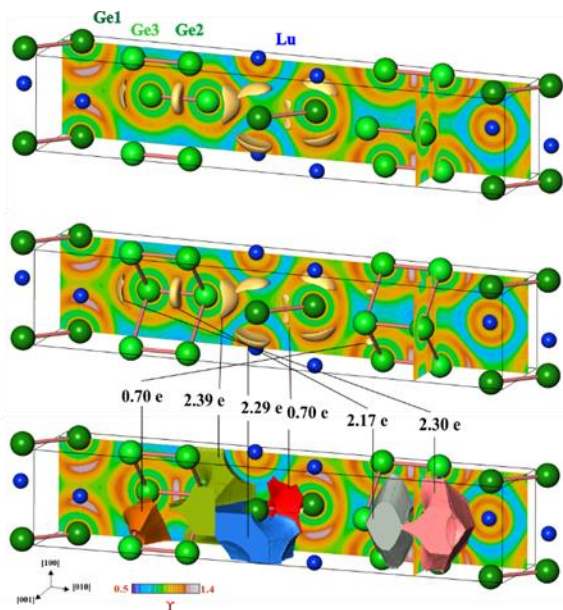


Figure-4: Electron localizability indicator in LuGe_3 : (top) Zintl-like arrangement of the attractors around the germanium atoms; (middle) $\text{Ge}_2\text{-Ge}_3$ interaction in the (010) planes; (bottom) bond basin populations.

The specific heat $C_p(T)$ of LuGe_3 at low temperatures indicates a critical temperature of $T_c = 3.1$ K. The value for the electronic specific heat C_e of the superconducting state $2 \Delta_0 / k_B T_c = 3.87$ is in accordance with that of 3.52 for weak coupling in the BCS theory. The value for the jump of C_e at T_c , $\Delta C_e / \gamma_N T_c = 1.43$ is also in almost perfect agreement with the BCS value of 1.44. Thus, experimental data consistently indicate that LuGe_3 belongs to the group of weakly coupled superconductors.

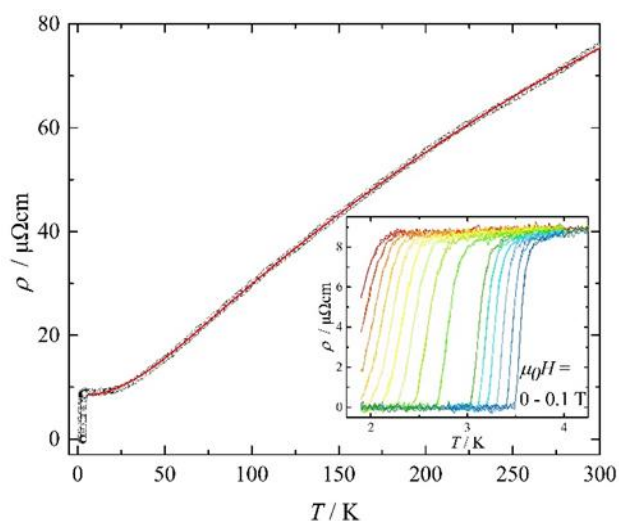


Figure-5: Electrical resistivity of LuGe_3 at zero-field, solid red line represents the fit to the Bloch-Grüneisen expression. Inset: Low-temperature electrical resistivity of LuGe_3 in $\mu_0H = 0$ to 0.1 T.

The spectrum of methods for tailoring the properties of covalent intermetallic compounds is frequently quite restricted as chemical substitution often causes structure changes. In these cases, the influence of the modified spatial arrangement adds to the effects of doping. Here, we present the example of the binary compound SrAl_4 and the ternary SrAl_4 -type solid solution $\text{SrAl}_{4-x}\text{Si}_x$ for $x = 1$ and 2 . The formation of the tetragonal high-pressure phases SrAl_3Si_1 and SrAl_2Si_2 was observed between 6 to 9.5 GPa using temperatures ranging from 400 to 1250 °C.

The site preference of the neighbouring elements Al and Si in the crystal structure of SrAl_2Si_2 cannot be determined by X-ray diffraction. Insight into the ordering of the network atoms is provided by ^{27}Al and ^{29}Si NMR spectroscopy using magic-angle spinning measurements. The observed signals in SrAl_2Si_2 indicate full ordering, i.e., Al and Si each occupy a single crystallographic site (see report [Bobnar](#)).

The interatomic interactions in the parent compound and the substituted variants are investigated by direct-space bonding analysis with the electron localizability indicator (ELI-D) for SrAl_4 , SrAl_3Si , and SrAl_2Si_2 (Figure 6).

In SrAl_4 , two types of bonding maxima are located between the aluminium atoms. The associated basins contain 2.05 and 1.41 electrons each, consistent with a 2-centre-2-electron picture for the interlayer bonds and electron-deficient 2-centre bonding within the layers. In SrAl_3Si , the additional electrons contribute preferentially to the bonding within the $[\text{Al}_3\text{Si}_1]$ layers. Finally, in SrAl_2Si_2 we find two distinct maxima indicating separated layers and lone pairs. Each lone pair basin contains 2.04 electrons, while the Al-Si bonding basins within the layers contain 1.41 electrons each.

At low temperatures, SrAl_2Si_2 exhibits a transition into a superconducting state with a critical temperature of approximately 2.6 K. The magnetic susceptibility of SrAl_2Si_2 exhibits a zero-field-cooled superconducting diamagnetic response which is close to complete, indicating bulk superconductivity. The Meissner effect is much weaker, presumably due to a strong flux line pinning, indicating a type-II superconductor. Samples with lower Si content (SrAl_4 , $\text{SrAl}_{3.5}\text{Si}_{0.5}$ and SrAl_3Si) do not exhibit superconductivity.

Outlook

The presented examples demonstrate that using the parameter pressure in synthesis paves the way for

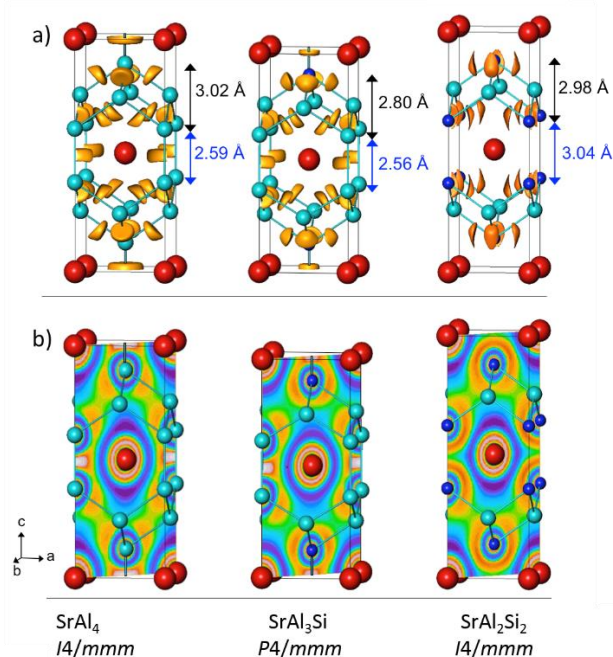


Figure-6: Crystal structure and chemical bonding in $\text{SrAl}_{4-x}\text{Si}_x$ [4]. (a) Electron localizability indicator (ELI-D) isosurfaces with an ELI-D value of 1.4 (1.36 for SrAl_3Si) show the positions of the attractors within the Al and Si network. Note that the Si–Si bond in SrAl_3Si is visible using a lower isosurface value. (b) ELI-D distributions in (200) planes. The Al₄ and Al₃Si slabs are interconnected by covalent bonds while the Al₂Si₂ layers are separated [4].

manufacturing novel covalent intermetallic compounds. These comprise atoms in often unusual local environments, setting the stage for exotic bonding features and intriguing physical properties. Thus, the parameter pressure can help to overcome existing limitations of preparative chemistry, granting access to hitherto blank areas on the map of binary intermetallic compounds.

External Cooperation Partners

W. Clarke, R. Niewa (Universität Stuttgart, Germany); S. Steinberg, R. Dronskowski (RWTH Aachen, Germany); C. McCammon, M. Bykov, L. Dubrovinsky (BGI Universität Bayreuth, Germany); I. Kupenko (ESRF Grenoble, Frankreich); J.-T. Zhao (University Shanghai, China)

References

- [1] *High-Pressure NiAs-Type Modification of FeN*, W.P. Clark, S. Steinberg, R. Dronskowski, C. McCammon, I. Kupenko, M. Bykov, L. Dubrovinsky, L. G. Akselrud, U. Schwarz and R. Niewa, *Angewandte Chemie Int. Ed.* **56** (2017) 7302, <https://doi.org/10.1002/anie.201702440>.

- [2] *Weak interactions under pressure: hp-CuBi and its analogues*, K. Guo, L. Akselrud, M. Bobnar, U. Burkhardt, M. Schmidt, J.-T. Zhao, U. Schwarz and Y. Grin, *Angewandte Chemie Int. Ed.* **56**,(2017) 5620, <https://doi.org/10.1002/anie.201700712>.
- [3] *High-pressure synthesis of the new binary superconductor lutetium trigermanide, LuGe₃*, J. Hübner, M. Bobnar, Y. Prots, U. Schwarz and Y. Grin, *Z. Kristallogr. Suppl.* **18** (2018) 11.
- [4] *Making and Breaking Bonds in Superconducting SrAl_{4-x}Si_x (0 ≤ x ≤ 2)*, A. Zevalkink, M. Bobnar, U. Schwarz and Y. Grin, *Chem. Mater.* **29**, (2017) 1236, <https://doi.org/10.1021/acs.chemmater.6b04615>.

schwarz@cpfs.mpg.de